Kinetics and Catalysis, Vol. 46, No. 4, 2005, pp. 509–515. Translated from Kinetika i Kataliz, Vol. 46, No. 4, 2005, pp. 543–549.

Prediction of Comparative Catalytic Activity in the Series of Single Crystalline Surfaces in a Water-Gas Shift Reaction

A. V. Zeigarnik*, C. Callaghan, R. Datta**, I. Fishtik**, and E. Shustorovich*****

** Zelinskii Institute of Organic Chemistry, Russian Academy of Sciences, Moscow, 119991 Russia*

*** Fuel Cell Center, Department of Chemical Engineering, Worcester Polytechnic Institute, 100 Institute Road, Worcester, MA 01609-2280, USA*

**** American Scientific Materials Technologies, Inc., 485 Madison Avenue, 24th Floor, New York, NY 10022, USA*

Received June 18, 2003

Abstract—A method is proposed for predicting comparative catalytic activity. This method includes the following stages: (1) formulation of a general reaction mechanism that is applicable to the whole series of catalysts, (2) calculation of the Arrhenius activation energies and the preexponential factors, and (3) kinetic simulations for the preset conditions. The method is illustrated by the model water-gas shift reaction (WGSR) $CO + H_2O = CO_2 + H_2$ and a series of catalytic single crystalline surfaces Cu(111), Ag(111), Au(111), Ni(111), Pd(111), Pt(111), and Fe(110). The mechanism is formulated using the computer program MECHEM. The activation energies are calculated using the UBI–QEP method. The reaction kinetics is simulated for a plug-flow reactor. The following series of the catalytic activity is obtained: Cu(111) > Ni(111) > Fe(111) > Pt(111), Pd(111) > Ag(111) > Au(111).

INTRODUCTION

Predicting the activity in a series of similar catalysts has always been an interesting problem in catalytic chemistry. The practical computational solution of this problem inevitably meets various computational difficulties. However, for some relatively simple systems, these difficulties can be overcome. In this study, we propose the following method to solve the problem. At the first stage, it is necessary to formulate a general reaction mechanism that is applicable to all catalysts in the series. Computer programs capable of generating complete lists of the elementary steps and intermediate species are convenient for accomplishing this stage [1–3]. At the second stage, the activation energy should be calculated for each step and the preexponential factor of the Arrhenius equation should be chosen or calculated. It is impractical to perform these calculations at the *ab initio* level given the present state of modern theory and computer technology. Therefore, empirical methods are preferable. At the third stage, the reaction kinetics should be simulated for any specific given conditions. As a result of these simulations, one can judge the most active catalyst and the comparative catalytic activity in the series.

To test the applicability of the method proposed, we chose the water-gas shift reaction (WGSR)

$$CO + H_2O = CO_2 + H_2,$$

and a series of single crystalline surfaces Cu(111), Ag(111), Au(111), Ni(111), Pd(111), Pt(111), and Fe(110).

COMPUTATIONAL METHODS

Stage 1: Generation of the Reaction Mechanism

To generate the reaction mechanism, we used the MECHEM computer program, which makes it possible to obtain the complete set of elementary reactions for a given set of initial, intermediate, and product species. The program is capable of solving more complex problems, such as the generation of the complete set of reaction pathways, and does not require all species to be preset [2–4]. However, in this case we solved the simplest task. The following species were taken as input: H_{ads}, O_{ads}, OH_{ads}, H_2O_{ads}, $H_{2,\,ads}$, CO_{ads}, $CO_{2,\,ads}$, $HCOO_{ads}$, and 14 reversible reactions were the output:

$$H_{2,\,ads} = H_{ads} + H_{ads}, \quad \text{(I)}$$

$$H_2O_{ads} = H_{ads} + OH_{ads}, \quad \text{(II)}$$

$$CO_{2,\,ads} = CO_{ads} + O_{ads}, \quad \text{(III)}$$

$$HCOO_{ads} = CO_{ads} + OH_{ads}, \quad \text{(IV)}$$

$$OH_{ads} = O_{ads} + H_{ads}, \quad \text{(V)}$$

$$CO_{2,\,ads} + H_{ads} = CO_{ads} + OH_{ads}, \quad \text{(VI)}$$

$$HCOO_{ads} = CO_{2,\,ads} + H_{ads}, \quad \text{(VII)}$$

$$CO_{2,\,ads} + OH_{ads} = HCOO_{ads} + O_{ads}, \quad \text{(VIII)}$$

$$H_2O_{ads} + O_{ads} = OH_{ads} + OH_{ads}, \quad \text{(IX)}$$

$$H_2O_{ads} + H_{ads} = OH_{ads} + H_{2,\,ads}, \quad \text{(X)}$$

$$O_{ads} + H_{2,\,ads} = OH_{ads} + H_{ads}, \quad \text{(XI)}$$

$$CO_{2,\,ads} + H_2O_{ads} = HCOO_{ads} + OH_{ads}, \quad \text{(XII)}$$

0023-1584/05/4604-0509 © 2005 MAIK “Nauka/Interperiodica”

$$CO_{2,\,ads} + H_{2,\,ads} = HCOO_{ads} + H_{ads}, \quad \text{(XIII)}$$

$$H_2O_{ads} = H_{2,\,ads} + O_{ads}. \quad \text{(XIV)}$$

The last reaction was excluded from this set, because it did not look elementary and had a hypothetical transition state that is too complex. We also found that, if this step is included in the mechanism, the results of kinetic simulations become inconsistent with experimental data. The above set of reactions was supplemented with adsorption–desorption steps:

$$H_2O_g = H_2O_{ads}, \quad \text{(XV)}$$

$$CO_g = CO_{ads}, \quad \text{(XVI)}$$

$$CO_{2,\,g} = CO_{2,\,ads}, \quad \text{(XVII)}$$

$$H_{2,\,g} = H_{2,\,ads}. \quad \text{(XVIII)}$$

Stage 2: Calculation of the Activation Energies of Elementary Steps

To calculate the activation energies of elementary reactions we used the unity bond index–quadratic exponential potential (UBI–QEP) [5–7]. This method has been used to obtain information on various heterogeneous catalytic reactions: methanol synthesis [8–10], dry reforming of methane [11], ethane hydrogenolysis [12, 13], acetylene hydrogenation [14], methanol oxidation to formaldehyde [15], CO hydrogenation [16], Fischer–Tropsch synthesis [17, 18], decomposition and reduction of NO [19], ammonia synthesis [20], decomposition of N_2O [21], and many others. The UBI–QEP method accepts as input the binding energies of adsorbed species on metal surfaces, that were determined in experiments by reliable theoretical methods.

When calculating the activation energies, the binding energies of adsorbates are first determined. The latter are calculated from the energies of two-center metal–element bond energies (Q_0). These bond energies are assumed to be constants and can be taken from [22]. Thus, the following formula is used to calculate the binding energies of H and O (Q_H and Q_O) on the cited surfaces,

$$Q_A = Q_0(2 - 1/n), \quad (1)$$

where $n = 3$, A = H, O. To calculate the binding energy of OH, the following formula is used:

$$Q_{OH} = \frac{Q_O^2}{Q_O + D_{OH}}, \quad (2)$$

where D_{OH} is the O–H bond dissociation energy (102 kcal/mol). To calculate the binding energy of H_2O, the following formula is used:

$$Q_{H_2O} = \frac{Q_{0,\,O}^2}{Q_{0,\,O} + D_{H_2O}}, \quad (3)$$

where D_{H_2O} is the sum of bond dissociation energies in H_2O (221 kcal/mol). The binding energy of H_2 is calculated by the formula

$$Q_{H_2} = \frac{9Q_{0,\,H}^2}{6Q_{0,\,H} + 16D_{H_2}}, \quad (4)$$

where D_{H_2} is the H–H bond dissociation energy (104 kcal/mol). For the CO molecule, the UBI–QEP method does not provide reliable information. Therefore, we used the experimental values of binding energies. For the CO_2 molecule, the best approximation seems to be a model according to which the O=C=O fragment is replaced by the O···O fragment, and the pseudobond energy $D_{O\cdots O}$ is considered equal to the sum of bond energies in CO_2 (384 kcal/mol). The binding energy is calculated by a formula analogous to formula (4) with $Q_{O,\,O}$ in place of $Q_{O,\,H}$ and $D_{O\cdots O}$ in place of D_{H_2}. There are alternative calculation methods [22], but they all give very close values of binding energies. The binding energy of HCOO is calculated by the formula

$$Q_{HCOO} = 1.5\frac{Q_O^2}{Q_O + D_{CO}}, \quad (5)$$

where D_{CO} is the C–O bond dissociation energy (166 kcal/mol). Here, chelating binding is considered [5, 6].

In the calculations of the activation energies, we used standard UBI–QEP formulas [5, 6]. For reactions of the type

$$AB_{ads} \longrightarrow A_{ads} + B_{ads} \quad \text{(XIX)}$$

the following formula for the activation energy is used:

$$E = \frac{1}{2}\left(\Delta H + \frac{Q_A Q_B}{Q_A + Q_B}\right), \quad (6)$$

where ΔH is the enthalpy of the surface reaction calculated from the thermodynamic cycle desorption–gas-phase reaction–adsorption:

$$\Delta H = Q_{AB} + D - Q_A - Q_B. \quad (7)$$

In this equation, D is the enthalpy of the analogous gas-phase reaction estimated from the bond dissociation energies:

$$D = D_{AB} - D_A - D_B. \quad (8)$$

The activation energy of the reverse is calculated from the condition

$$E_{reverse} = E_{forward} - \Delta H. \quad (9)$$

In the case of the dissociation of triatomic molecules, such as CO_2 and N_2O, formula (10) without a multiplier of 1/2 is used instead of formula (6) [5]:

$$E = \Delta H + \frac{Q_A Q_B}{Q_A + Q_B}. \quad (10)$$

If the activation energy is lower than zero, thermodynamic correction applies: this activation energy is set

Table 1. Species binding energies (kcal/mol) in WGSR and their comparison with literature data

Species	Metal													
	Cu(111)		Ag(111)		Au(111)		Ni(111)		Pd(111)		Pt(111)		Fe(110)	
	calculated	reference data	calculated	reference data	calculated	reference data	calculated	reference data	calculated	reference data	calculated	reference data	calculated	reference data
H_{ads}	56.0	–	52.0	–	46.0	–	63.0	–	62.0	–	61.0	–	66.0	–
O_{ads}	103.0	–	80.0	–	75.0	–	115.0	–	87.2	–	85.0	–	125.0	–
OH_{ads}	51.8	–	35.2	55 [30]	31.8	–	60.9	–	40.2	60 [31]	38.6	60 [32, 35]	68.8	–
H_2O_{ads}	13.5	9.8 [29]	8.6	9–10 [30]	7.6	–	16.4	10–12 [34–36]	10.0	–	9.6	9.6 [37]	19.0	–
$H_{2,\,ads}$	5.4	–	4.7	–	3.7	–	6.8	–	6.6	–	6.4	–	7.4	–
CO_{ads}	–	12.0 [38]*	–	6.5 [40]	–	7.0**	–	27.0***	–	34.0***	–	32.0***	–	36.0 [18]
$CO_{2,\,ads}$	5.3	–	3.2	–	2.8	–	6.5	–	3.8	–	3.6	–	7.7	–
$HCOO_{ads}$	59.2	54.5 [42]	39.0	–	35.0	–	70.6	–	45.0	–	43.2	–	80.5	–

Note: Data on the binding energies of O and H were taken from the literature or obtained by correlations; therefore, it makes no sense to compare them with literature data. There are no reference data for CO_2 and H_2, because these species bind in the molecular state very weakly, and experimental data are not available.

*The value taken from [38]. There are also data in [39], where seven different values, ranging from 10.7 to 13.3 kcal/mol, are discussed.

**DFT data [41]. This value seems to be an overestimate, but the UBI–QEP method gives even higher values.

***There are many inconsistent data for these surfaces [12, 13, 39]; here, the value that was tested in other calculations [6] is taken.

equal to zero, and the activation energy of the reverse reaction is chosen so that Eq. (9) is valid.

The activation energy of a reaction of the type

$$A_{ads} + BC_{ads} \longrightarrow AB_{ads} + C_{ads} \qquad (XX)$$

is calculated using the following formulas:

$$E = \frac{1}{2}\left(\Delta H + \frac{Q_{AB}Q_C}{Q_{AB} + Q_C}\right). \qquad (11)$$

$$\Delta H = Q_A + Q_{BC} + D_{BC} - D_{AB} - Q_{AB} - Q_C. \qquad (12)$$

The "correct" direction from the standpoint of the UBI–QEP method is chosen so that the condition for the corresponding bond energies $D_{BC} > D_{AB}$ is met. Using formulas (1)–(12), we calculated the binding energies for all species and the activation energies of elementary steps on the surfaces Ni(111), Pd(111), Pt(111), Ag(111), Au(111), Cu(111), and Fe(110). Tables 1 and 2 summarize the results of these calculations.

The reliability of data obtained for single crystalline surfaces is evident from comparison with experimental and cutting edge theoretical data reported by other researchers (Table 1). As can be seen, there is good agreement between the results of UBI–QEP calculations and literature data. However, a difference of ~20 kcal/mol is observed for the OH species. The reason for this discrepancy is the formation of OH islands due to hydrogen bonds even at low surface coverage. These bonds are neglected by the UBI–QEP method [23]. If the value of Q_{H_2O} is increased by 20 kcal/mol for all metals, we obtain other values of the activation energies; they are listed in Table 3. In this study, we carried out kinetic simulations for the two sets of activation energies (Tables 2, 3).

Stage 3: Kinetic Simulation of WGSR

In kinetic simulations we used the same preexponential factors as in [24]. These were estimated by transition state theory [25]. As in [26], we assumed that the preexponential factors are 10 Pa^{-1} s^{-1} for adsorption steps and 10^{13} s^{-1} for surface reactions. Then, the preexponential factors were refined for the adsorption and desorption steps taking into account the thermodynamics of the overall reaction

$$\sum_j \sigma_j E_{\text{forward},\,j} - \sum_j \sigma_j E_{\text{reverse},\,j} = \Delta H^0 \qquad (13)$$

and

$$\prod_j \left(\frac{A_{\text{forward},\,j}}{A_{\text{reverse},\,j}}\right)^{\sigma_j} = \exp\left(\frac{\Delta G^0 - \Delta H^0}{RT}\right), \qquad (14)$$

where ΔH^0 and ΔG^0 are the enthalpy and the Gibbs energy of the overall reaction, respectively; σ_j is the Horiuti stoichiometric number of the jth step; $E_{\text{forward},\,j}$ and $E_{\text{reverse},\,j}$ are the activation energies of the jth step in the forward and reverse directions, respectively; and $A_{\text{forward},\,j}$ and $A_{\text{reverse},\,j}$ are the corresponding preexponential factors. Then, we used the same preexponential factors for all metal surfaces:

Adsorption-desorption step	$A_{\text{forward},\,j}$	$A_{\text{reverse},\,j}$
$H_2O_g = H_2O_{ads}$	10^6	10^{14}
$CO_g = CO_{ads}$	10^6	10^{14}
$CO_{2,\,g} = CO_{2,\,ads}$	10^6	4×10^{12}
$H_{2,\,g} = H_{2,\,ads}$	10^6	6×10^{12}

Table 2. The activation energies (kcal/mol) of steps in the forward (left column) and reverse (right column) directions in WGSR obtained without correcting the Q_{OH} values (see simulation data in Fig. 2)

Step		Metal													
		Cu(111)		Ag(111)		Au(111)		Ni(111)		Pd(111)		Pt(111)		Fe(110)	
		for.	rev.	for.	rev.	for.	rev.	for.	rev.	for.	rev.	for.	rev.	for.	rev.
$H_2O_g = H_2O_{ads}$	(XV)	0	13.5	0	8.6	0	7.6	0	16.4	0	10.0	0	9.6	0	19.0
$CO_g = CO_{ads}$	(XVI)	0	12.0	0	6.5	0	7.0	0	27.0	0	34.0	0	32.0	0	36.0
$CO_{2,\,g} = CO_{2,\,ads}$	(XVII)	0	5.3	0	3.2	0	2.8	0	6.5	0	3.8	0	3.6	0	7.7
$H_{2,\,ads} = H_{ads} + H_{ads}$	(I)	12.7	15.3	15.4	10.6	19.4	3.6	8.2	23.3	8.8	22.2	9.5	21.0	6.2	26.8
$H_{2,\,g} = H_{2,\,ads}$	(XVIII)	0	5.4	0	4.7	0	3.7	0	6.8	0.0	6.6	0	6.4	0	7.4
$H_2O_{ads} = H_{ads} + OH_{ads}$	(II)	25.8	1.1	40.4	0	48.8	0	21.2	9.8	26.8	0	28.9	0	18.4	15.3
$CO_{2,\,ads} = CO_{ads} + O_{ads}$	(III)	28.0	10.7	49.7	6.0	54.2	6.4	13.4	21.9	34.1	24.5	36.9	23.2	1.6	28.0
$HCOO_{ads} = CO_{ads} + OH_{ads}$	(IV)	20.4	0	22.3	0	21.2	0	13.2	5.5	7.1	11.3	7.5	10.0	12.2	11.5
$OH_{ads} = O_{ads} + H_{ads}$	(V)	15.5	20.8	18.3	13.2	20.6	7.9	12.8	27.9	14.6	21.6	15.1	20.4	11.5	31.7
$CO_{2,\,ads} + H_{ads} = CO_{ads} + OH_{ads}$	(VI)	22.5	0	38.5	0	35.1	0	12.6	6.1	17.5	0.9	19.0	0	8.7	14.9
$HCOO_{ads} = CO_{2,\,ads} + H_{,ads}$	(VII)	1.4	3.5	0	16.2	0	13.8	3.5	2.4	0	20.8	0	21.5	6.9	0
$CO_{2,ads} + OH_{ads} = HCOO_{ads} + O_{ads}$	(VIII)	17.2	20.4	23.8	2.4	26.6	0	13.8	29.9	21.7	7.9	22.4	6.3	11.0	38.0
$H_2O_{ads} + O_{ads} = OH_{ads} + OH_{ads}$	(IX)	30.0	0	35.2	0	36.1	0	28.5	2.0	33.8	0	34.3	0	28.9	5.5
$H_2O_{ads} + H_{ads} = OH_{ads} + H_{2,\,ads}$	(X)	27.3	0	35.7	0	33.1	0	26.7	0	40.2	0	40.5	0	23.7	0
$O_{ads} + H_{2,\,ads} = OH_{ads} + H_{ads}$	(XI)	14.8	12.1	10.3	10.7	10.9	7.9	15.4	15.6	9.0	15.4	8.7	14.9	16.6	17.1
$CO_{2,\,ads} + H_2O_{ads} = HCOO_{ads} + OH_{ads}$	(XII)	27.2	0.4	56.6	0	62.7	0	21.6	11.1	47.6	0	50.4	0	16.7	20.4
$CO_{2,\,ads} + H_{2,\,ads} = HCOO_{ads} + H_{ads}$	(XIII)	14.2	14.6	21.6	0.7	29.6	0	8.5	24.8	16.7	9.3	17.6	7.7	4.4	31.9

The reaction kinetics was simulated using the equations for a plug-flow reactor:

$$\frac{dx_i}{dt} = \frac{1}{\tau}(x_i^0 - x_i) + \frac{1-\varepsilon}{\varepsilon}\frac{RT}{P}\frac{C_t S_t \rho_{cat}}{N_A}\sum_{j=1}^{p}\beta_{ji} r_j \quad (15)$$

for $i = H_2O$, CO, H_2, and CO_2,

$$\frac{d\theta_k}{dt} = \sum_{j=1}^{p}\alpha_{jk} r_j \quad (16)$$

for species on the catalyst surface.

Here, x_i^0 and x_i are the molar fractions of H_2O, CO, CO_2, and H_2 at the inlet and outlet of the reactor; the concentrations at the reactor inlet were taken equal to 20, 15, 5, and 5%, respectively; the balance was inert (nitrogen); τ is the contact time (0.1 s); ε is the catalyst porosity assumed to be equal to 0.5; C_t is the active site density on the catalyst surface (1.9×10^{15} cm^{-2}); S_t is the specific surface area of the catalyst (3.6×10^5 cm^2/g); N_A is the Avogadro number; and ρ_{cat} is the density of the catalyst (2.5 g/cm^3). The numeric values are chosen rather arbitrarily and can be changed if necessary.

Equations (15) and (16) were solved numerically in the Berkley Madonna environment, which was developed for the analysis of dynamic systems [27].

Kinetic modeling of WGSR on the Cu(111) surface using the first set of data (Table 2) showed that this procedure leads to good agreement between simulated and experimental data for this surface [24].

RESULTS AND DISCUSSION

As noted above, we examined two sets of activation energies. The first set (Table 2) gives the results that agree well with the experiment [24], whereas the second set contains more accurate binding energies of OH (Table 3) [23]. Let us consider the first of these.

The conversion of CO at various temperatures was taken as an activity measure (Fig. 1). As can be seen from this figure, the shapes of all curves are similar: at low temperatures the reaction does not occur, then the light-off is observed and the conversion shortly reaches the equilibrium value. As expected, the lowest light-off temperature is seen for the copper surface, which is the most active at 320–500 K. The next active metal is nickel. At temperatures higher than 520 K, its activity becomes higher than the activity of copper and other catalysts. At ~600 K the light-off is observed for the iron surface and at 640 K the activity of iron becomes higher than the activity of copper. The palladium and platinum surfaces behave similarly and are the least active. According to the results obtained, silver and gold surfaces are almost completely inactive, which is mainly due to the high activation energy of the bond cleavage in a water molecule on the surfaces of these metals.

Table 3. The activation energies (kcal/mol) of steps in the forward (left column) and reverse (right column) directions in WGSR obtained with the correction for the Q_{OH} values (see simulation data in Fig. 2)

Step		Metal													
		Cu(111)		Ag(111)		Au(111)		Ni(111)		Pd(111)		Pt(111)		Fe(110)	
		for.	rev.	for.	rev.	for.	rev.	for.	rev.	for.	rev.	for.	rev.	for.	rev.
$H_2O_g = H_2O_{ads}$	(XV)	0	13.5	0	8.6	0	7.6	0	16.4	0	10.0	0	9.6	0	19.0
$CO_g = CO_{ads}$	(XVI)	0	12.0	0	6.5	0	7.0	0	27.0	0	34.0	0	32.0	0	36.0
$CO_{2,\,g} = CO_{2,\,ads}$	(XVII)	0	5.3	0	3.2	0	2.8	0	6.5	0	3.8	0	3.6	0	7.7
$H_{2,\,ads} = H_{ads} + H_{ads}$	(I)	12.7	15.3	15.4	10.6	19.4	3.6	8.2	23.3	8.8	22.2	9.5	21.0	6.2	26.8
$H_{2,\,g} = H_{2,\,ads}$	(XVIII)	0	5.4	0	4.7	0	3.7	0.0	6.8	0	6.6	0	6.4	0	7.4
$H_2O_{ads} = H_{ads} + OH_{ads}$	(II)	18.1	13.3	23.6	3.2	28.8	0	13.4	22.0	18.7	11.8	19.4	10.5	10.5	27.3
$CO_{2,\,ads} = CO_{ads} + O_{ads}$	(III)	28.0	10.7	49.7	6.0	54.2	6.4	13.4	21.9	34.1	24.5	36.9	23.2	1.6	28.0
$HCOO_{ads} = CO_{ads} + OH_{ads}$	(IV)	5.3	4.9	4.1	1.8	3.7	2.5	3.9	16.3	0	24.1	0	22.5	3.2	22.5
$OH_{ads} = O_{ads} + H_{ads}$	(V)	25.5	10.8	28.3	3.2	32.8	0	22.8	17.9	24.6	11.6	25.1	10.4	21.5	21.7
$CO_{2,\,ads} + H_{ads} = CO_{ads} + OH_{ads}$	(VI)	6.4	3.9	18.5	0	15.1	0	3.4	16.8	9.2	12.5	9.8	10.9	0	26.2
$HCOO_{ads} = CO_{2,\,ads} + H_{ads}$	(VII)	1.4	3.5	0	16.2	0	13.8	3.5	2.4	0	20.8	0	21.5	6.9	0
$CO_{2,ads} + OH_{ads} = HCOO_{ads} + O_{ads}$	(VIII)	27.2	10.4	41.4	0	46.6	0	23.8	19.9	33.8	0	36.1	0	21.0	28.0
$H_2O_{ads} + O_{ads} = OH_{ads} + OH_{ads}$	(IX)	12.9	22.9	11.4	16.2	11.0	14.9	13.5	27.0	12.0	18.1	11.8	17.5	13.9	30.5
$H_2O_{ads} + H_{ads} = OH_{ads} + H_{2,\,ads}$	(X)	7.3	0	15.7	0	13.1	0	6.7	0	20.2	0	26.3	5.8	5.3	1.6
$O_{ads} + H_{2,\,ads} = OH_{ads} + H_{ads}$	(XI)	7.1	24.4	3.2	23.6	3.7	20.7	7.6	27.8	2.1	28.5	1.8	28.1	8.7	29.1
$CO_{2,\,ads} + H_2O_{ads} = HCOO_{ads} + OH_{ads}$	(XII)	19.6	12.8	36.6	0	42.7	0	14.1	23.6	27.6	0	30.4	0	9.3	33.0
$CO_{2,\,ads} + H_{2,\,ads} = HCOO_{ads} + H_{ads}$	(XIII)	14.2	14.6	21.6	0.7	29.6	0	8.5	24.8	16.7	9.3	17.6	7.7	4.4	31.9

Thus, for each temperature, one can construct an activity series of surfaces. For instance, at 510 K, the activity series is as follows:

$$Cu \gg Ni > Fe > Pd, Pt \gg Ag, Au.$$

Unfortunately, this activity series cannot be compared with experimental data, because no comparative experimental study of the single crystalline surfaces discussed in this work has been carried out. Comparison with real catalytic systems would be incorrect, because there are many factors that affect the activity of real catalytic systems (involvement of various single crystalline facets in the catalytic process, the nature of the support, the presence of defects, etc.). Nevertheless, some correlations are seen. Thus, it was reported in [28] that the activity series for metals supported on Al_2O_3 (at 573 K) is

$$Cu \gg Ni \gg Pt > Fe \sim Pd,$$

which differs somewhat from our series obtained for single crystalline surfaces.

For the second set of activation energies (Table 3), we obtained analogous temperature dependences of CO

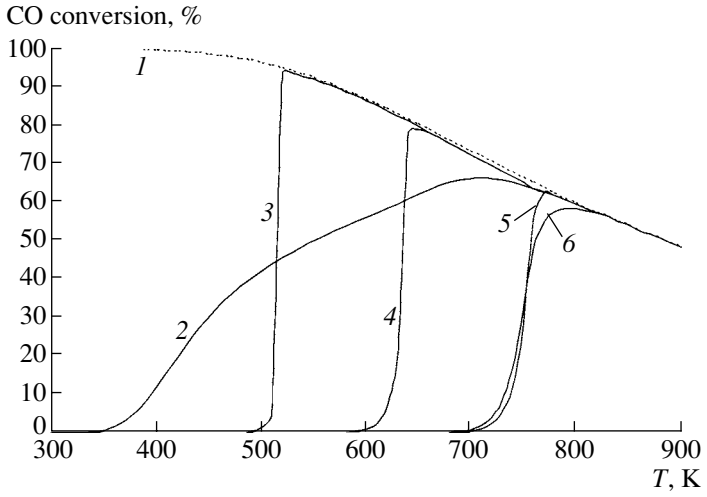

Fig. 1. Conversion of CO at different temperatures in (*1*) equilibrium and various surfaces: (*2*) Cu(111); (*3*) Ni(111); (*4*) Fe(110); (*5*) Pd(111); (*6*) Pt(111). Data of Table 2 are used.

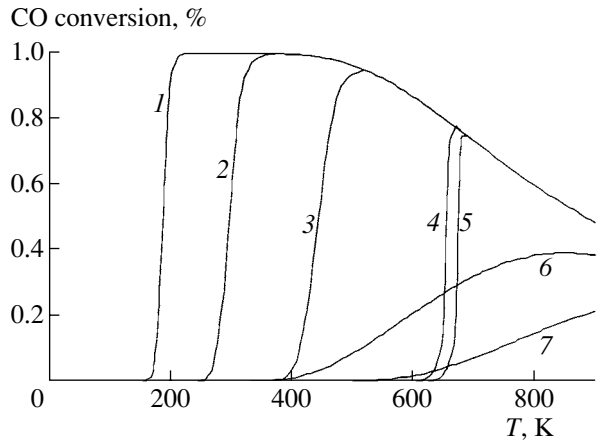

Fig. 2. Conversion of CO at different temperatures in equilibrium and various surfaces: (*1*) Cu(111); (*2*) Ni(111); (*3*) Fe(110); (*4*) Pt(111); (*5*) Pd(111), (*6*) Ag(111); (*7*) Au(111). Data of Table 3 are used.

conversion (Fig. 2). Although the initial data used in kinetic simulations agree better with the experiment, the results of simulations are quantitatively not as good. For instance, on the Cu(111) surface, the complete conversion of CO is achieved at room temperature, which defies common sense. However, if the comparative activity is considered at the qualitative level, we obtain results similar to those obtained for the first set of activation energies. If we judge the activity by the light-off temperatures, the activity series remains the same:

$$\text{Cu} > \text{Ni} > \text{Fe} > \text{Pt,Pd} > \text{Ag} > \text{Au}.$$

At the qualitative level, we obtain the same results regardless of the set of initial data. Note that the correction introduced for the Q_{OH} value reflects a change from the zero-coverage approximation to nonzero coverage. However, hydrogen bonds are only one of the factors in such a change. There is a factor that has an opposite effect: a decrease in the binding energies with increasing surface coverage due to coadsorption. We conjecture that Q_{OH} should vary with coverage in the range between the uncorrected zero-coverage value and the corrected one. On the other hand, the binding energies of other adsorbates and the related activation energies are also coverage-dependent, which is neglected in our simulations. Therefore, a quantitative agreement with experiment should not be expected. The qualitative agreement with experiment is good for the sets of coverage-independent activation energies.

CONCLUSIONS

In this work, we proposed a method for predicting catalytic activity and illustrated its use for the WGSR and a series of single crystalline surfaces. The method includes the generation of the complete set of elementary steps using a computer program (e.g., MECHEM), the calculation of the activation energies by the UBI–QEP method and the preexponential factors using transition state theory, and kinetic simulations. The UBI–QEP method does not always provide accurate and reliable data on the activation energies, and transition state theory is not always accurate in estimating the preexponential factors, but there is no doubt that new, more accurate procedures for finding such estimates for real catalytic systems will be developed soon. The proposed theoretical method will then be able to point us in the right direction in experimental catalyst selection.

REFERENCES

1. Zeigarnik, A.V., Bruk, L.G., Temkin, O.N., Likholobov, V.A., and Maier, L.I., *Usp. Khim.*, 1996, vol. 65, p. 125.
2. Zeigarnik, A.V., Valdes-Perez, R.E., and White, B.S., *J. Chem. Educ.*, 2000, vol. 77, p. 214.
3. Zeigarnik, A.V., Valdes-Perez, R.E., and Temkin, O.N., *Langmuir*, 1998, vol. 14, p. 4510.
4. Valdes-Perez, R.E. and Zeigarnik, A.V., *J. Mol. Catal., A: Chem.*, 1997, vol. 119, p. 405.
5. Shustorovich, E., *Adv. Catal.*, 1990, vol. 37, p. 101.
6. Shustorovich, E. and Sellers, H., *Surf. Sci. Rep.*, 1998, vol. 31, p. 1.
7. Sellers, H. and Shustorovich, E., *Surf. Sci.*, 2002, vol. 504, p. 167.
8. Shustorovich, E. and Bell, A., *Surf. Sci.*, 1991, vol. 253, p. 386.
9. Paredes Olivera, P., Patrito, E.M., and Sellers, H., *Surf. Sci.*, 1995, vol. 327, p. 330.
10. Wang, G., Zhao, Y., Cai, Z., Pan, Y., Zhao, X., Li, Y., San, Y., and Zong, B., *Surf. Sci.*, 2000, vol. 465, p. 51.
11. Hei, M.J., Chen, H.B., Yi, J., Lin, Y.J., Lin, Y.Z., Wei, G., and Liao, D.W., *Surf. Sci.*, 1998, vol. 417, p. 82.
12. Zeigarnik, A.V., Valdes-Perez, R.E., and Myatkovskaya, O.N., *J. Phys. Chem. B*, 2000, vol. 104, p. 10578.
13. Zeigarnik, A.V. and Myatkovskaya, O.N., *Kinet. Katal.*, 2001, vol. 42 [*Kinet. Catal.* (Engl. Transl.), vol. 42, p. 418].
14. Gislason, J., Xia, W., and Sellers, H., *J. Phys. Chem. A*, 2002, vol. 106, p. 767.
15. Shen, B., Chen, X., Fan, K., and Deng, J.-F., *Surf. Sci.*, 1998, vol. 408, p. 128.
16. Bell, A. and Shustorovich, E., *J. Catal.*, 1990, vol. 121, p. 1.
17. Shustorovich, E. and Bell, A., *Surf. Sci.*, 1991, vol. 248, p. 359.
18. Shustorovich, E., *Catal. Lett.*, 1990, vol. 7, p. 107.
19. Shustorovich, E. and Bell, A., *Surf. Sci.*, 1993, vol. 289, p. 127.
20. Shustorovich, E. and Bell, A., *Surf. Sci.*, 1991, vol. 259, p. L791.
21. Zeigarnik, A.V., *Kinet. Katal.*, 2003, vol. 44, p. 250 [*Kinet. Catal.* (Engl. Transl.), vol. 44, p. 233].
22. Shustorovich, E. and Zeigarnik, A.V., *Surf. Sci.*, 2003, vol. 527, p. 137.
23. Patrito, E.M., Paredas Olivera, P., and Sellers, H., *Surf. Sci.*, 1994, vol. 306, p. 447.

24. Fishtik, I. and Datta, R., *Surf. Sci.*, 2002, vol. 512, p. 229.
25. Dumesic, J.A., Rudd, D.F., Aparicio, L.M., Rekoske, J.E., and Trevino, A.A., *The Microkinetics of Heterogeneous Catalysis*, Washington, DC: ACS, 1993.
26. Waugh, K.C., *Catal. Today*, 1999, vol. 53, p. 161.
27. www.berkeleymadonna.com.
28. Grenoble, D.C., Estadt, M.M., and Ollis, D.F., *J. Catal.*, 1981, vol. 67, p. 90.
29. Campbell, C.T. and Daube, K.A., *J. Catal.*, 1987, vol. 104, p. 109.
30. Bange, K., Madey, T.E., Sass, J.K., and Stuve, E.M., *Surf. Sci.*, 1987, vol. 183, p. 334.
31. Anderson, L.C., Mooney, C.E., and Lunsford, J.H., *Chem. Phys. Lett.*, 1992, vol. 196, p. 445.
32. Fujimoto, G.T., Selwyn, G.S., Kelser, J.T., and Lin, M.C., *J. Phys. Chem.*, 1983, vol. 87, p. 1906.
33. Anton, A.B. and Cadogan, D.C., *Surf. Sci.*, 1980, vol. 239, p. 587.
34. Thiel, P.A. and Madey, T.E., *Surf. Sci. Rep.*, 1987, vol. 7, p. 211.
35. Stulen, R.H. and Thiel, P.A., *Surf. Sci.*, 1985, vol. 157, p. 99.
36. Madey, T.E. and Netzer, F.P., *Surf. Sci.*, 1982, vol. 117, p. 549.
37. Sexton, B.A. and Huges, A.E., *Surf. Sci.*, 1984, vol. 140, p. 227.
38. Hollins, P. and Pritchard, J., *Surf. Sci.*, 1979, vol. 89, p. 486.
39. Christoffersen, E., Stoltze, P., and Norskov, J.K., *Surf. Sci.*, 2002, vol. 505, p. 200.
40. McElhiney, G., Papp, H., and Pritchard, J., *Surf. Sci.*, 1976, vol. 54, p. 617.
41. Mavrikakis, M., Stoltze, P., and Norskov, J.K., *Catal. Lett.*, 2000, vol. 64, p. 101.
42. Gomes, J.R.B. and Gomes, J.A.N.F., *Surf. Sci.*, 2001, vol. 471, p. 59.